Site-Directed Mutagenesis of Residues within Helix VI in Subunit I of the Cytochrome bo_3 Ubiquinol Oxidase from *Escherichia coli* Suggests That Tyrosine 288 May Be a Cu_B Ligand†

Jeffrey W. Thomas,‡ Melissa W. Calhoun,‡ Laura J. Lemieux,‡,§ Anne Puustinen,∥ Mårten Wikström,∥ James O. Alben,⊥ and Robert B. Gennis*,‡

School of Chemical Sciences, University of Illinois, Urbana, Illinois 61801, Helsinki Bioenergetics Group, Department of Medical Chemistry, University of Helsinki, P.O. Box 8, SF-00014, Helsinki, Finland, and Department of Medical Biochemistry, Ohio State University, Columbus, Ohio 43210

Received May 18, 1994; Revised Manuscript Received August 22, 1994®

ABSTRACT: The heme–copper oxidase superfamily contains all of the mammalian mitochondrial cytochrome *c* oxidases, as well as most prokaryotic respiratory oxidases. All members of the superfamily have a subunit homologous to subunit I of the mammalian cytochrome *c* oxidases. This subunit provides the amino acid ligands to a low-spin heme component as well as to a heme–copper binuclear center, which is the site where dioxygen is reduced to water. The amino acid sequence of transmembrane helix VI of subunit I is the most highly conserved within the superfamily. Previous efforts have demonstrated that one of the residues in this region, H284, is critical for oxidase activity and for the assembly of Cu_B. This paper presents the analysis of additional site-directed mutants in which other highly conserved residues in helix VI (P285, E286, Y288, and P293) have been substituted. Most of the mutants are enzymatically inactive. Structural perturbations reported by Fourier transform infrared absorption difference spectroscopy of CO adducts of the mutant oxidases confirm the previous suggestion that this region is adjactent to Cu_B. Furthermore, the analysis of five different substitutions for Y288 indicates that all lack Cu_B. On the basis of these data, it is proposed that Y288 may be a Cu_B ligand along with H333, H334, and H284, and a plausible molecular model of the Cu_B site is presented.

The cytochrome bo_3 ubiquinol oxidase from *Escherichia coli* is a member of the superfamily of heme–copper oxidases[1] that share a common structure and function (Hosler et al., 1993). All of the respiratory oxidases in this superfamily, which includes the mammalian aa_3-type cytochrome *c* oxidases, contain a low-spin heme and binuclear metal center, which consists of a high-spin heme in close proximity to a copper atom (Cu_B) (Hill et al., 1992; Hosler et al., 1993; Shapleigh et al., 1992a). The heme–Cu_B binuclear center is the site of oxygen binding. All of the enzymes in this superfamily catalyze the 4-electron reduction of dioxygen to water and use the free energy available from this reaction to pump protons across the membrane (Krab & Wikström, 1978; Minghetti & Gennis, 1988; Minghetti et al., 1992; Solioz et al., 1982; Sone & Hinkle, 1982; Wikström, 1977; Wikström & Krab, 1979). The energy from the resulting proton gradient is utilized to drive cellular processes such as ATP synthesis.

Examination of amino acid sequence alignments indicates a high degree of sequence homology among the heme–copper oxidases, with subunit I displaying the highest level of conservation (Saraste, 1990). By using site-directed mutants in both the *E. coli* cytochrome bo_3 and *Rb. sphaeroides* cytochrome aa_3 oxidases, the six conserved histidine residues in subunit I have been assigned as metal ligands to the two hemes and Cu_B (Calhoun et al., 1993a–c; Lemieux et al., 1992; Minagawa et al., 1992; Shapleigh et al., 1992b). It should be noted that, in the cytochrome *c* oxidases, a second copper-binding site (Cu_A) is located in subunit II (Kelly et al., 1993; Lappalainen et al., 1993; Saraste, 1990).

The application of site-directed mutagenesis has recently contributed important strutural and functional information concerning the heme–copper oxidases (Calhoun et al., 1993a–c; Hosler et al., 1993; Lemieux et al., 1992; Lemon et al., 1993; Uno et al., 1994). The cytochrome bo_3 ubiquinol oxidase from *E. coli* has been the subject of most of these studies because this system is amenable to genetic manipulations as well as spectroscopic and biochemical studies. Site-directed mutants in subunit I have been the focus of much of this work. This subunit contains all of the redox machinery in the cytochrome bo_3 ubiquinol oxidase (Hosler et al., 1993). Many of the residues in subunit I are highly conserved among the nearly 80 sequences currently available for subunit I variants from different species (Saraste, 1990; M. W. Calhoun, unpublished). Gene fusion experiments (Chepuri & Gennis, 1990) have shown that subunit I in the *E. coli* oxidase contains 15 transmembrane helices (Figure 1). Twelve of these transmembrane helices (I–XII, Figure 1) are common to all members of the heme–copper oxidase superfamily. The three additional transmembrane helices (0, XIII, and XIV; Figure 1) are present in several of the bacterial oxidases (Ishizuka et al., 1990; Santana et al., 1992). The six conserved histidines

† This work was supported by grants from the U.S. Department of Energy (to R.B.G., DE-FG-02-87ER13716), the National Science Foundation (to J.O.A., DMB89-04614), the Sigrid Juselius Foundation (to M.W.), and the Academy of Finland (MRC).

‡ University of Illinois.

§ Current address: Department of Pathology, Richardson Laboratory, Queen's University, Kingston, Ontario, Canada K7L 3N6.

∥ University of Helsinki.

⊥ Ohio State University.

® Abstract published in *Advance ACS Abstracts,* October 1, 1994.

[1] Due to the diversity of heme groups utilized in the heme–copper oxidases, the nomenclature can be confusing. For the purpose of this paper, the following conventions will be used. In the cytochrome bo_3 ubiquinol oxidase from *E. coli*, the low-spin heme center will be referred to as heme *b* and the oxygen-binding heme as heme o_3. In the cytochrome *c* oxidases, the low-spin heme will be referred to as heme *a* and the oxygen-binding heme as heme a_3. Amino acid sequence numbers will be those of cytochrome bo_3 from *E. coli* unless noted otherwise.

0006-2960/94/0433-13013$04.50/0

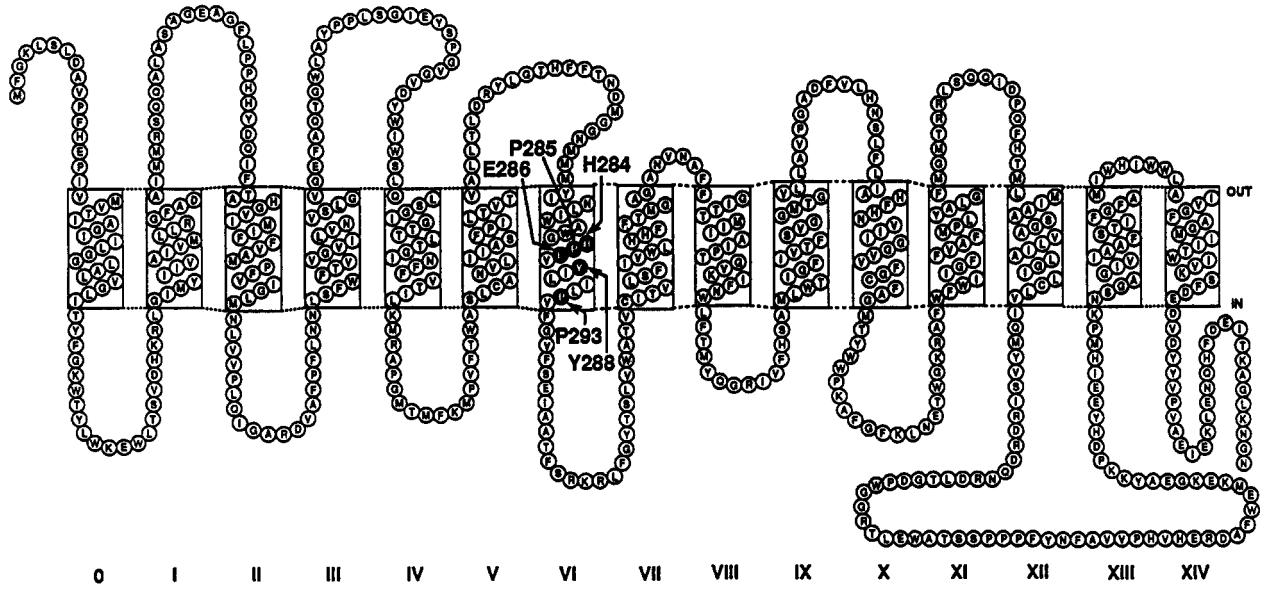

FIGURE 1: Two-dimensional topological model of subunit I of the bo_3-type ubiquinol oxidase from *E. coli*. The highly conserved polar residues in helix VI are highlighted.

that have been implicated as metal ligands are located in four of the transmembrane helices: H106 (helix II), H284 (helix VI), H333 and H334 (helix VII), and H419 and H421 (helix X). Previous data have indicated that H106 and H421 ligate the low-spin heme *b* (Lemieux et al., 1992; Minagawa et al., 1992). H419 ligates the high-spin heme o_3 in the binuclear center (Calhoun et al., 1993b,c; Uno et al., 1994), and H333, H334, and probably H284 ligate Cu_B (Calhoun et al., 1993a,c). The model that has resulted from these ligand assignments makes the prediction that transmembrane helix VI, which is the most highly conserved region in the entire superfamily (Saraste, 1990), is adjacent to Cu_B and is on the distal side of the high-spin heme o_3. The work presented in this paper is designed to test this model.

Site-directed mutagenesis was used to make substitutions for several highly conserved amino acid residues in helix VI (P285G, E286A, Y288A, -C, -F, -H, and -S, and P293A). The results are consistent with the model, insofar as several of the mutations appear to selectively perturb Cu_B. Most importantly, all of the substitutions for Y288 appear to lack Cu_B, similar to the results previously obtained with the H284 mutations. Molecular modeling shows that it is possible to have Cu_B located between helices VI and VII and ligated with tetrahedral coordination to H333, H334 (helix VII), and H284 and Y288 (helix VI). It is proposed that Y288 may be a Cu_B ligand.

MATERIALS AND METHODS

The mutants were constructed and sequences verified according to Lemieux et al. (1992) and Thomas et al. (1993a). Y288F and Y288S are in the plasmid pL3, and Y288A is in the plasmid pMC31 (Lemieux et al., 1992). P285G, E286A, Y288C, Y288H, and P293A are in the plasmid pJT39 (Thomas et al., 1993b). Mutant plasmids were transformed into the host strain GL101 (*cyo*, *sdh*, *rec*A), and cells were grown for spectroscopic analysis according to Lemieux et al. (1992), except that the growth medium was supplemented with 100 μg/mL $CuSO_4$. UV–visible spectra were acquired as noted previously (Lemieux et al., 1992).

Mutant plasmids were transformed into the host strain RG129 (*cyo*, *cyd*, *rec*A) for complementation, activity, and proton pumping assays. Protocols for these assays were as listed previously (Chepuri et al., 1990; Lemieux et al., 1992; Puustinen et al., 1989, 1991; Thomas et al., 1993a).

Fourier transform infrared (FTIR) spectra were recorded according to previously published protocols (Hill et al., 1991, 1992; Shapleigh et al., 1992a). FTIR sample preparation and instrument conditions were similar to those noted in Shapleigh et al. (1992a) and Thomas et al. (1993a,b) and are summarized here. Crude membranes (Lemieux et al., 1992) containing cytochrome bo_3 in the host strain GL101 were used to prepare the reduced CO adduct for FTIR. One milliliter of membranes isolated from approximately 1 L of cells was suspended in 15 mL of 50 mM Tris-HCl (pH 7.5) with 67 mM lactate added. The 60Ti centrifuge tubes were then sealed by a rubber septum. The tubes were then made anaerobic by flushing argon through them. One milliliter of 1.0 M sodium dithionite, previously made anaerobic, was added to the tubes followed by additional flushing with argon. CO was added by passing CO gas over the samples for 10 min. Under a flow of CO, the tube was sealed with the appropriate centrifuge cap, and then the sample was pelleted at 150000*g* for 2 h. Again under a flow of CO, the supernatant was decanted and CO-saturated glycerol was added to dehydrate the membrane sample. The tubes were purged with CO, and the caps were replaced. The sample was kept at 4 °C for a minimum of 4 h.

A portion of the sample was placed between two CaF_2 windows (Janos Technology, Inc.) and pressed to an appropriate thickness. A Mattson Sirius 100 FT-IR interferometer equipped with a Lake Shore Cryotronics closed-cycle helium refrigerator and a liquid nitrogen cooled indium antimonide detector was used to record the FTIR spectra. Interferograms were detected in the single-beam mode and presented as a light minus dark absorbance difference spectrum with a resolution of 0.5 cm^{-1}. The dark spectrum was recorded before photolysis. The light spectrum was recorded during continuous irradiation of the sample by a 500 W tungsten bulb filtered through glass and water. The light and dark spectra are the average of 512 scans collected at low (10–25 K) or high (120–135 K) temperatures. Subtraction of the least-squares fits of a cubic polynomial to the baseline regions of the spectra was used for baseline correction on the E286A FTIR spectrum at 135 K and the Y288F FTIR spectrum at 20 K. There was no further averaging, smoothing, or other correction to the spectra. Spectra taken at 135 K were also recorded under identical conditions. The same sample was used at both temperatures. The samples were warmed to 210

Table 1: Complementation Data for the Cytochrome bo_3 Mutants in Helix VI of Subunit I

	complementation[a]
wild-type	+
Pro285Gly	−
Glu286Ala	−
Tyr288Ala	−
Tyr288Cys	−
Tyr288Phe	−
Tyr288His	−
Tyr288Ser	−
Pro293Ala[b]	+

[a] Complementation in a mutant is defined as the ability to support aerobic growth as the sole oxidase on a nonfermentable substrate in the RG129 host strain. [b] Pro293Ala has ubiquinol oxidase specific activity equal to that of the wild-type. This mutant also has proton pumping activity similar to that of the wild-type ($H^+/e^- \sim 2$ at pH 7).

K for 10 min after each photolysis and data collection to allow the carbon monoxide (CO) to relax back to heme o_3 in the binuclear center.

A model of the ligation of the Cu_B site utilizing helix VI and helix VII (Calhoun et al., 1993a–c; Holm et al., 1987; Lemieux et al., 1992; Minagawa et al., 1992; Shapleigh et al., 1992b) was first assembled using a Minit molecular model kit (Cochranes of Oxford, Oxford, U.K.). To test the validity of this stick model, a computer model was generated using the HyperChem program (Autodesk, Inc.). The modeling was based on fully reduced copper and was done both with and without (not shown) CO ligated to Cu_B. The structures were geometrically optimized by use of the MM^+ force field and the steepest descent method of energy minimization (100–150 cycles were applied to each model). A bond length of approximately 2 Å between the metal and the ligand was chosen as an acceptable distance, on the basis of the bond lengths in other copper proteins (Chakrabarti, 1990). The $N\epsilon_2$ nitrogens of H284, H333, and H334 were used in the test for ligation, as a prior compilation demonstrated that helical histidines bind metal ions only through the $N\epsilon_2$ nitrogen (Chakrabarti, 1990). The same study suggested that coordination of the metal through $N\delta_1$ of a histidine would place the metal so close to the helix that it would prevent coordination by another residue (Chakrabarti, 1990).

RESULTS

Several highly conserved amino acid residues in helix VI of subunit I from the cytochrome bo_3 ubiquinol oxidase were mutated to probe their role in the structure and function of the enzyme. As shown in Table 1, P285G, E286A, Y288A, Y88C, Y288F, Y288H, and Y288S mutant enzymes cannot confer the ability to grow aerobically to an oxidase-deficient strain of *E. coli*. P293A is the only mutant in this set that complements for aerobic growth, and the ubiquinol oxidase specific activity of this mutant, measured in membrane preparations, is equivalent to that of the wild-type oxidase. Since proton pumping can be measured only for enzymatically active mutants, P293A was the only mutant for which this was evaluated. P293A was found to have an H^+/e^- ratio of 1.6–1.9 at pH 7, indicating that this mutant pumps protons as efficiently as the wild-type oxidase (Puustinen et al., 1989).

Figure 2A shows the dithionite-reduced minus air-oxidized visible difference spectra (measured at 77 K) of the membranes containing the overexpressed mutant enzymes. All of the mutants except Y288C have the characteristic split α band near 562 nm, indicating the presence of the low-spin heme *b* in each of these membrane preparations (Lemieux et al., 1992; Minghetti et al., 1992; Puustinen et al., 1991). Figure 2B shows the corresponding (dithionite-reduced plus CO) minus (dithionite-reduced) visible difference spectra recorded at room temperature. All of the mutants, except Y288C, bind CO to an extent similar to the wild-type oxidase, indicating the presence of the high-spin heme o_3. The Y288C mutant displays no evidence of either the low-spin heme or the high-spin heme and appears not to be assembled in the membrane. These data show that although seven of the eight mutants in this set are enzymatically inactive, all but one of these seven is assembled and present in the membrane to an extent comparable to the wild-type. These data were subjected to further spectroscopic characterization.

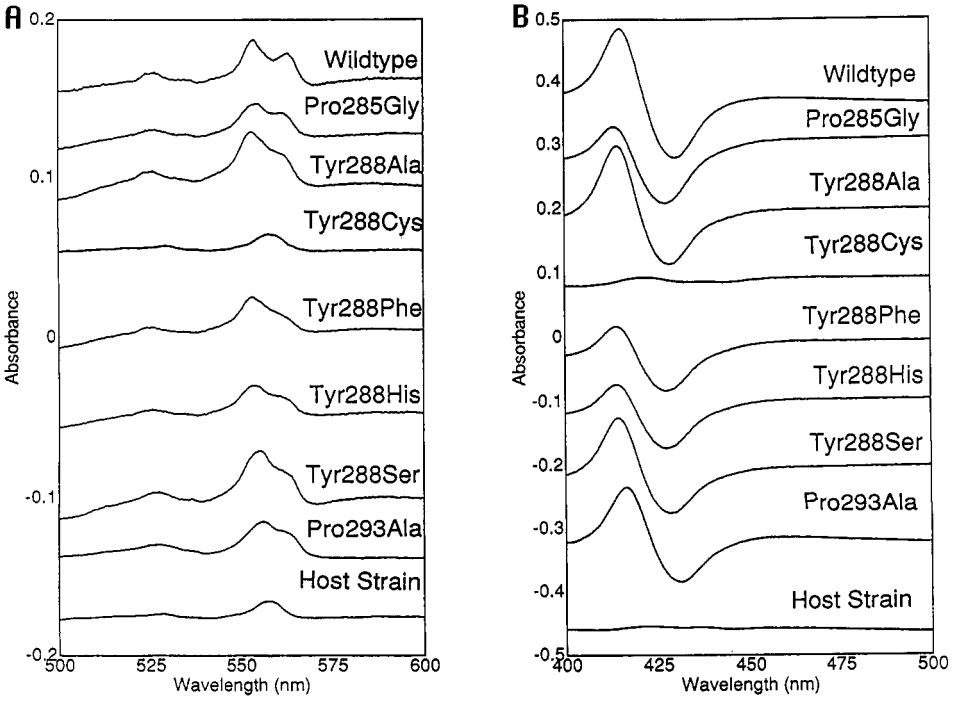

FIGURE 2: (A) α region of the dithionite-reduced minus air-oxidized visible spectra at 77 K for the noted mutants in helix VI. The split α peak at 562 nm is diagnostic for the low-spin heme center. (B) Soret region of the dithionite-reduced plus CO minus dithionite-reduced visible spectrum at room temperature for the noted mutants.

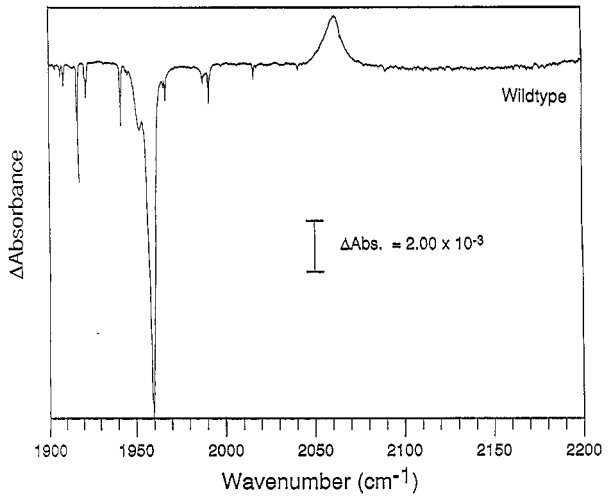

FIGURE 3: FTIR difference spectrum of wild-type cytochrome bo_3-type oxidase from *E. coli* at 20 K. The Fe–CO center frequency is at 1959.8 cm^{-1}, and the Cu_B–CO center frequency is at 2061.6 cm^{-1}. Sample thickness is 27 μm.

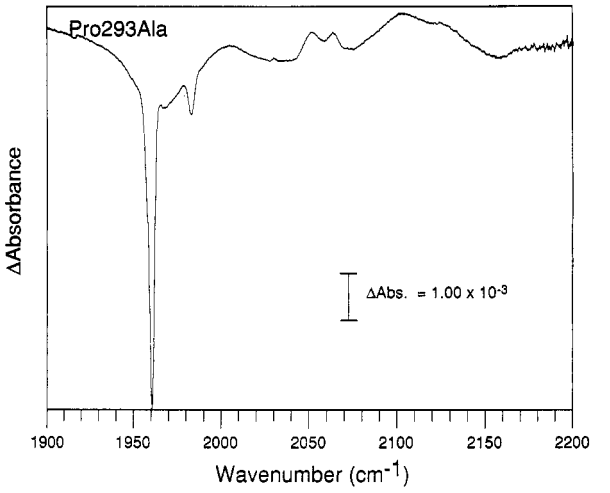

FIGURE 4: FTIR absorbance difference spectrum of the P293A mutant at 20 K. The conditions are similar to those described for Figure 3. The features are those of the wild-type (Figure 3), with the exception that the band attributed to the Cu_B–CO adduct is split with distinct peaks at 2051 and 2063 cm^{-1}. The Fe–CO band of the cytochrome *bd* is at 1983 cm^{-1}.

To further probe the structure of the binuclear center of each mutant, Fourier transform infrared (FTIR) absorbance difference spectra of the CO adducts were recorded. In this technique, the stretching freqencies of CO bound to the metals in the binuclear center are used as a spectroscopic monitor of the environment provided by the binuclear center. The CO probe is sensitive to the environment of the binuclear center and produces characteristic bands in the wild-type enzyme. The reported spectra are the light minus dark absorbance difference FTIR spectra. In the dark spectrum, the CO probe is bound to the heme o_3 Fe. Upon photolysis (light spectrum), the CO photodissociates from the heme Fe and binds to Cu_B. Under cryogenic conditions ($T < 140$ K), the CO remains bound to Cu_B for long periods of time (i.e., hours or days) (J. J. Hill, R. B. Gennis, & J. O. Alben, manuscript in preparation). The FTIR absorbance difference spectrum of the wild-type oxidase in the *E. coli* membrane is shown in Figure 3 for comparison to the spectra of the mutants. The Fe–CO and the Cu–CO bands are centered at 1960 and 2062 cm^{-1}, respectively. Perturbation to the binuclear center pocket can result in the broadening, shifting, addition, or deletion of bands to the FTIR spectrum (Calhoun et al., 1993a–c; Fiamingo et al., 1982, 1990; Hill et al., 1992; Thomas et al., 1993a).

The spectrum of the P293A mutant at 20 K is similar to that of the wild-type oxidase, except that the Cu–CO band clearly is split to an extent not seen with the wild-type (Figure 4). Instead of a single peak at 2062 cm^{-1}, a second Cu_B–CO peak appears at 2052 cm^{-1}. Hence, although this proline is very highly conserved in the heme–copper oxidase superfamily, its substitution by an alanine results in no measureable functional perturbation and only a subtle, but significant, change in the environment sensed by CO bound to Cu_B. In contrast, substitution of a glycine for P285 has more dramatic effects.

The FTIR difference spectrum of P285G (Figure 5A) at 14 K has two sharp Fe–CO bands at 1954 and 1960 cm^{-1}. This suggests the possibility that the P285G oxidase exists in two distinct conformations. The narrow bandwidth of each peak is indicative of a highly ordered pocket surrounding the heme o_3–CO adduct in each population. The band at 1984 cm^{-1} is the Fe–CO band from cytochrome *bd*, the alternate quinol oxidase in *E. coli* that is also present in these membrane preparations at low temperatures (14 K), but exhibits rapid geminate recombination with heme *d* and is not observed at

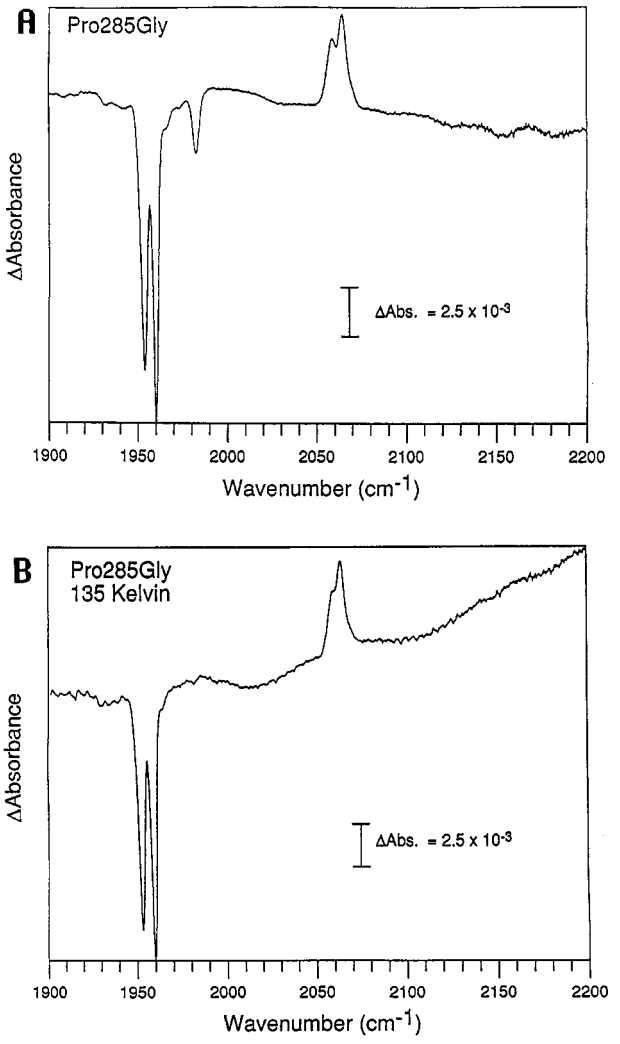

FIGURE 5: FTIR absorbance difference spectra of P285G (path length 38 μm) (A) at 14 K. The Fe–CO bands have center frequencies at 1954 and 1960 cm^{-1}. The Cu_B–CO bands are at 2059 and 2064 cm^{-1}. (B) Spectrum from A at 135 K. Fe–CO frequencies are at 1953 and 1960 cm^{-1}, and the Cu_B–CO bands are at 2060 and 2065 cm^{-1}.

higher temperatures (e.g., 135 K) (Hill et al., 1993). The P285G mutant has a clearly split Cu_B–CO band with peaks at 2064 and 2059 cm^{-1}. The baseline in this spectrum shows

broad variations associated with instrumental differences between sample and reference spectra. Maintenance of a constant environment is critical to obtain a flat baseline at this scale expansion.

An FTIR difference spectrum was also taken at 135 K (Figure 5B). If Cu_B is absent or does not bind to CO, then following photolysis at sufficiently low temperatures (e.g., 20 K), the CO will be weakly associated with the protein. At higher temperatures, the CO rapidly relaxes back to the high-spin heme Fe (Fiamingo et al., 1986). As a result, the peaks in the heme Fe–CO region that are due to heme species that are not stabilized by a corresponding copper component are subtracted out in FTIR difference spectra collected above 100 K. Hence, to determine whether both Fe–CO components in the FTIR difference spectrum of the P285G mutant have corresponding copper components, the spectrum was taken at 135 K.

At 135 K, Fe–CO bands remain (Figure 5B), indicating that each of the heme o_3–CO conformations represented by these two bands is associated with Cu_B. The data are consistent with the P285G mutation resulting in an assembled binuclear center that can exist in two distinct conformations. This mutation clearly perturbs both the heme Fe and copper environments. Note that the Fe–CO band at 1984 cm^{-1} (Figure 5A) arising from the alternate *E. coli* oxidase, cytochrome *bd* (Hill et al., 1993), disappears at 135 K (Figure 5B) due to the rapid recombination of CO back to the heme *d* Fe at this temperature.

When the spectrum of the P293A mutant is taken at 135 K, the amplitude of the high-frequency component of the Cu_B–CO band decreases (not shown). Such temperature-dependent shifts in the carbonyl polarization appear to reflect changes in protein conformation or hydrogen bonding (Fiamingo et al., 1990). As will be described later, a similar effect is observed with the E286A mutant.

The FTIR difference spectrum (Figure 6A) of the E286A mutant at 14 K appears to be wild-type in the Fe–CO region but is highly perturbed in the Cu–CO region, which contains three bands at 2052, 2063, and 2072 cm^{-1}. At 135 K (Figure 6B), the Cu_B–CO band at 2072 cm^{-1} merges with the 2063 cm^{-1} peak, but two distinct peaks remain. The mutation of E286 to alanine seems to affect the Cu_B environment while leaving the heme o_3 environment essentially wild-type. The mutation of E286 to glutamine (E286Q) has been shown previously to be fully active and to have an FTIR difference spectrum identical to that of the wild-type (Thomas et al., 1993b). As was seen previously in the spectra of membranes containing P285G, the 1984 cm^{-1} Fe–CO band from cytochrome *bd* is present at 14 K (Figure 6A), but is not observed at 135 K (Figure 6B).

The FTIR spectrum of Y288F at 20 K (Figure 7A) is representative of all of the substitutions at position 288, except for Y288C where no oxidase was assembled. The Fe–CO region of the spectrum (1940–1990 cm^{-1}) contains multiple highly broadened bands, indicating a highly disrupted environment around heme o_3. This mutant, as in all of the other mutations made for Y288, has no Cu–CO band at 2063 cm^{-1}, indicating that either Cu_B is absent or is not binding CO. At this low temperature, when Cu_B is not present, photodissociation of CO from the high-spin heme o_3 produces a CO–protein complex that absorbs in the region of 2130 cm^{-1} (Calhoun et al., 1993a,b; Thomas et al., 1993a). The FTIR difference spectrum of the Y288F mutant has bands in the 2124–2130 cm^{-1} region, indicating that CO–protein complexes form following photodissociation from heme o_3. To further support this finding, an additional spectrum at 120 K was

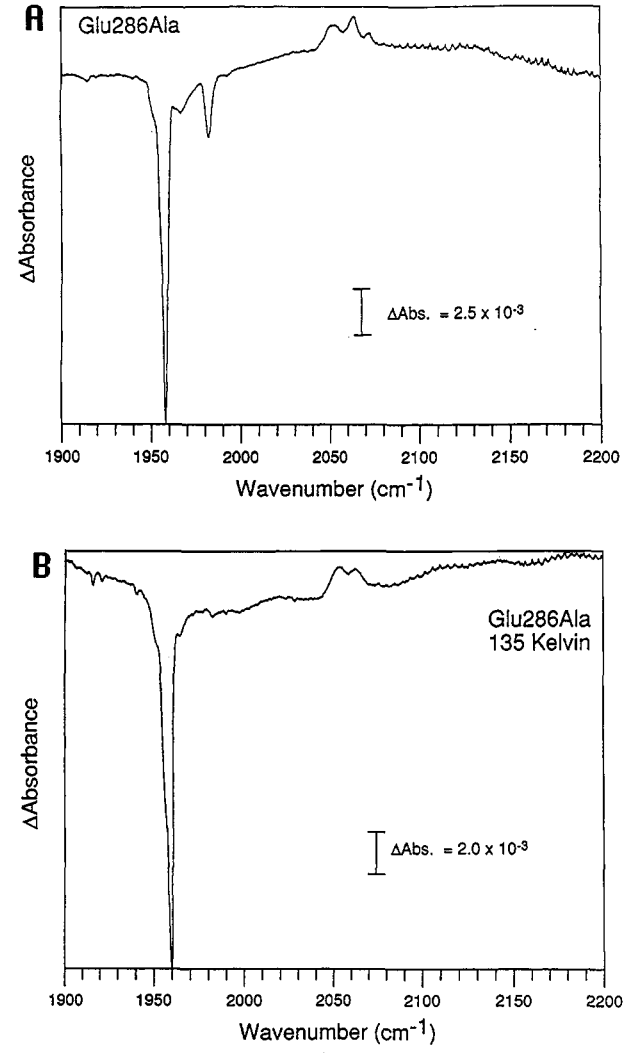

FIGURE 6: FTIR absorbance difference spectrum of E286A (path length 38 μm) (A) at 14 K. The Fe–CO stretch is at 1959 cm^{-1}, and the Cu_B–CO stretches are at 2052, 2063, and 2072 cm^{-1}. (B) Spectrum from A at 135 K. The Fe–CO band is at 1960 cm^{-1}, and the Cu_B–CO bands are at 2054 and 2063 cm^{-1}.

recorded (Figure 7B). The Y288F FTIR spectrum at 120 K results in the disappearance of the Fe–CO bands, supporting the conclusion that these heme species are not associated with a corresponding copper component. Note that the absorbance scale is 10-fold more sensitive in Figure 7B than that in Figure 7A, which is the same sample. The simplest interpretation is that Y288F lacks Cu_B. The other Y288 mutants (Y288A, -H, -S) also lack Cu_B by the same criterion (data not shown), suggesting the importance of this residue for the assembly or stable binding of Cu_B. It is important to note that all of these strains were grown with a copper supplement in the growth medium. Hence, the lack of Cu_B reflects a substantial effect and not a subtle change in the affinity of this site for binding to the metal.

The data from the current work, in combination with previous results implicating H333, H334, and H284 as potential Cu_B ligands (Calhoun et al., 1993a,c), suggest the possibility that all four residues might be Cu_B ligands. This would place Cu_B between helices VI and VII in the oxidase, as depicted in the helical wheel diagram in Figure 8. Previous modeling efforts have shown the feasibility of H333 and H334 ligating to Cu_B (Holm et al., 1987), and this has been supported recently by experimental work from this laboratory (Calhoun et al., 1993a).

Figure 9 shows the results of energy-minimized models of Cu_B, assuming H333, H334, H284, and Y288 as ligands.

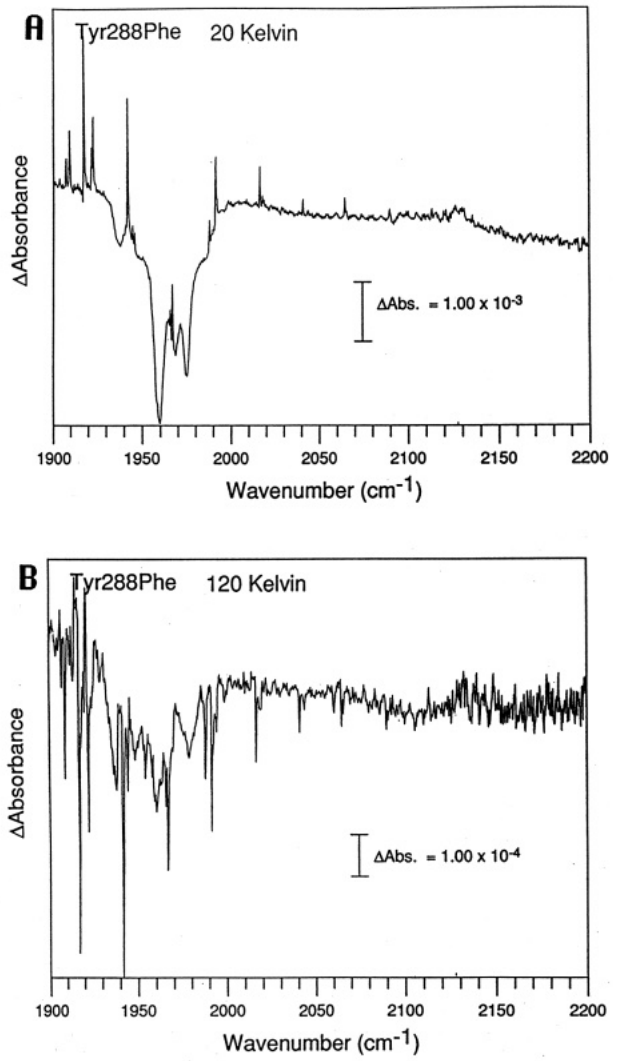

FIGURE 7: FTIR absorbance difference spectrum of Y288F (path length 24 μm) (A) at 20 K. The center frequencies for the Fe–CO bands are 1938, 1960, 1969, and 1975 cm^{-1}. (B) Spectrum from A at 120 K. The Fe–CO bands have nearly disappeared due to fast geminate recombination of the CO, since Cu_B is not present. The resulting spectrum is almost entirely background. Note the 10-fold enhanced scale in panel B.

Figure 9B shows the top down view of the site, whereas in Figure 9A the model includes CO bound to Cu_B and is viewed from the side. In the absence of CO, molecular modeling is consistent with tetrahedral geometry at the copper site with normal ligand-to-copper angles. The copper ion is depicted near the direction of the lone pair on the nitrogens of H284 ($N\epsilon_2$), H333 ($N\epsilon_2$), and H334 ($N\epsilon_2$), which is the common orientation for metal atoms ligated to histidines (Chakrabarti, 1990). The addition of CO (Figure 9A) favors trigonal bipyramidal geometry. The major point is that these ligation schemes are sterically possible.

DISCUSSION

The work presented in this paper has been designed to probe the structural and functional importance of residues within transmembrane helix VI in subunit I of the heme–copper oxidases. The amino acid sequence of this region of the protein, especially between W280 and P293, is the most highly conserved among the approximately 80 sequence variants of subunit I. Previous work both from both our laboratory (Calhoun et al., 1993c) and that of Anraku (Uno et al., 1994) has implicated H284 as being important for the assembly of Cu_B. The available evidence indicates that Cu_B is absent when H284 is replaced by any number of substitutions. At one

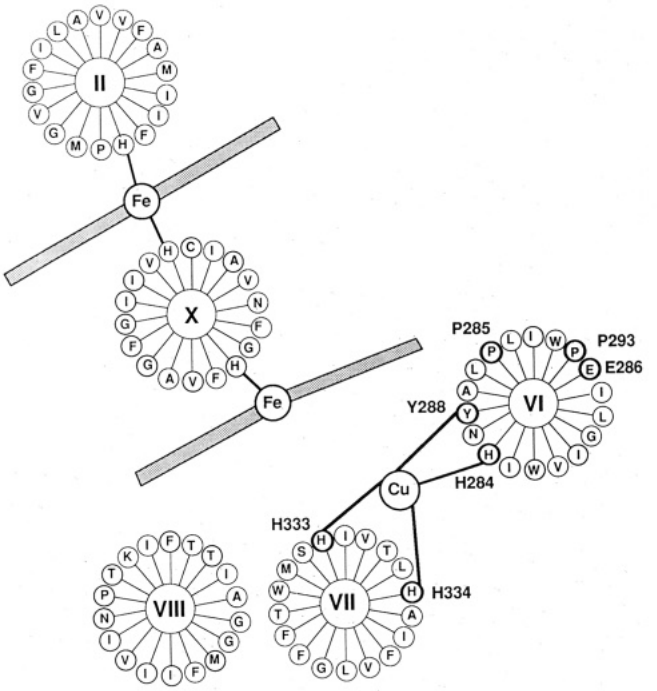

FIGURE 8: Helical wheel representation of the binuclear center pocket of the cytochrome bo_3-type oxidase from *E. coli* and, by analogy, that of the cytochrome aa_3-type oxidases. The conserved residues in helix VI are highlighted.

point, H284 was postulated to be the axial ligand to the high-spin heme component of the binuclear center (Shapleigh et al., 1992b), but experimental data (Calhoun et al., 1993c; Uno et al., 1994) have assigned this role to H419 in helix X. Hence, the current model (Figure 8) places helix VI on the distal side of the high-spin heme and adjacent to Cu_B in the binuclear center (Calhoun et al., 1993c; Hosler et al., 1993). The work in this paper is consistent with this model and, furthermore, suggests that Y288, located one helical turn below H284, is a particularly important residue and may be a Cu_B ligand.

Proline 293. This residue is one of two prolines that are present in helix VI in most of the sequences of subunit I. Of the residues examined in this work, P293 is predicted to be located nearest to the cytoplasmic side of the membrane, as shown in Figure 1. Substitution of an alanine at this position has no detrimental effect on either the quinol oxidase activity or the proton pumping function of the oxidase. Spectroscopically, the only alteration appears to be a clear splitting in the FTIR absorption difference band associated with the Cu_B–CO adduct (Figure 4). This appears to be the result of a subtle conformational effect at Cu_B and is qualitatively similar to the effects observed with the P285G and E286A mutations (Figures 5 and 6). The subtle alteration in the FTIR spectrum of the P293A mutant is confined to the Cu_B–CO adduct, and no similar splitting is observed in the heme Fe–CO adduct. This is consistent with the location of helix VI near Cu_B.

Proline 285. This residue is adjacent to H284, a putative Cu_B ligand (see Figures 8 and 9). Replacement by a glycine results in an inactive enzyme, as do substitutions for H284. However, whereas the substitutions for H284 appear to eliminate Cu_B (Calhoun et al., 1993c; Uno et al., 1994), the data shown in Figure 5 indicate that Cu_B is present in the P285G mutant. The clear split in the band associated with the absorbance of the Cu_B–CO adduct is similar to that observed with the P293A mutation (Figure 4). However, the spectrum of the P285G mutant suggests that the conformational alterations due to this mutation extend to the heme Fe–CO adduct, which is also split into two distinct peaks. The

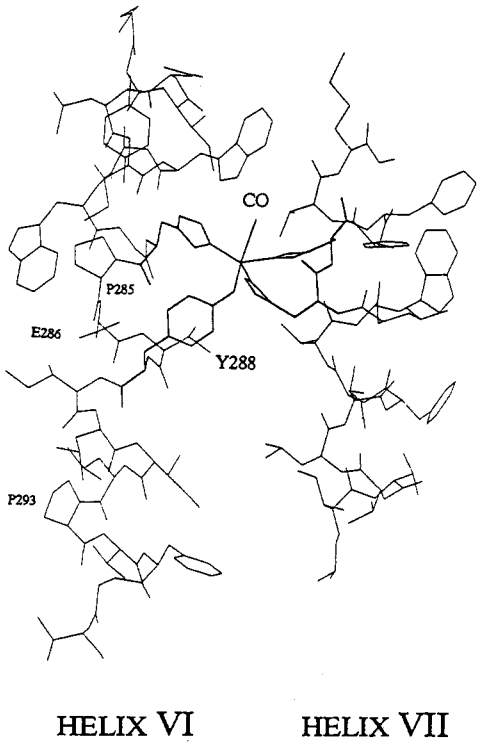

FIGURE 9: Computer-generated models of the ligation sphere of Cu_B by residues in transmembrane helices VI and VII. Part A shows a side view (perpendicular to the helix axes) of the fully reduced Cu_B center ligated to H333, H334, H284, and Y288, with bound CO. The geometry is distorted tetrahedral or trigonal bipyramidal. Ligation is represented as through the Nϵ2 nitrogens in all three histidines. Part B shows the end view of the model from part A.

protein in the vicinity of the binuclear center appears to exist in two different conformations in the P285G mutant. Unlike the P293A mutant, the P285G mutant is inactive. It is premature to claim that P285 is an essential residue for proper function, since only this one substitution has been examined. Two other highly conserved prolines located in putative transmembrane helices in subunit I, P293 (helix VI) (see above) and P358 (helix VIII) (Thomas et al., 1993a), can be altered without the loss of function. It is not unusual for membrane proteins to have prolines within transmembrane helices, and in several proteins a number of these prolines have been shown to be nonessential, for example, lactose permease, bacteriorhodopsin, and in the bc_1 complex (Ahl et al., 1988; Consler et al., 1991; Yun et al., 1992).

In molecular modeling (Figure 9), helix VI is maintained as a helix, but the effect of the two prolines is to introduce kinks that effectively cause helix VI to wrap around Cu_B. Such proline-induced helical bends have been observed in bacteriorhodopsin (Henderson et al., 1990). Clearly, however, P293 is not essential to maintain the structure, and P285G, although inactive, still binds to Cu_B. Possibly the proline is important due to the disruption of the normal backbone hydrogen-bonding patterns (Richardson & Richardson, 1990; Williams & Deber, 1991). Conceivably, this could be important in providing sites for bound water or otherwise providing a hydrogen-bonding network that is functionally important. However, additional mutations will be required to test whether P285 is truly essential.

Glutamate 286. E286 is the only highly conserved acidic residue that can reasonably be placed within a transmembrane span. The E286Q mutant was previously examined to test whether E286 plays a role in proton pumping analogous to the aspartates in bacteriorhodopsin (Henderson et al., 1990; Krebs & Khorana, 1993). This was shown not to be the case. The E286Q mutant is fully functional, and the FTIR absorption difference spectrum is identical to that of the wild-type (Thomas et al., 1993b). The result of placing a small nonpolar residue in this location is much more deleterious, however. The E286A mutant is enzymatically inactive, and the FTIR absorption difference spectrum shows perturbations specifically in the vicinity of the Cu_B–CO adduct. Although the band due to the heme Fe–CO is wild-type in character, the Cu_B–CO band is split into three distinct peaks (Figure 6). The data suggest that E286 may participate in an essential hydrogen bond interaction that requires a polar residue at this site (e.g., E286Q). The multiple conformations observed in the Cu_B–CO band of this mutant, and of P285G and P293A as well, could be the result of different hydrogen bond interactions with one or more of the ligands to Cu_B.

In previous work with bovine cytochrome *c* oxidase (Fiamingo et al., 1990), it was suggested that an 11 cm^{-1} spectral shift of the Cu_B–CO band upon the addition of ethanol was the result of disruption of a hydrogen bond with a ligand of Cu_B. At low temperatures, the band due to Cu_B–CO is split because the proposed hydrogen bond exchange is slower than the vibrational modes of the Cu_B–CO. At higher temperatures, the bands merge, indicating that the populations are in rapid equilibrium. In the FTIR spectrum of E286A at 14 K (Figure 7A), the Cu_B–CO band is split by 11 cm^{-1} (2052 and 2063 cm^{-1}). At 135 (Figure 7B) and 190 K (not shown), the Cu_B–CO bands in the E286A mutant begin to merge. As the temperature increases, the Cu_B–CO bands are less resolved, indicating more rapid interconversion of the subpopulations.

The origin of these subpopulations is unknown, but the narrow bands are indicative of a highly ordered and constrained binuclear pocket. If helix VI is indeed helical, as in the modeling shown in Figures 8 and 9, E286 would be expected to be facing away from the binuclear center, so that a hydrogen bond interaction with a Cu_B ligand is unlikely. However, one must consider the possibility that this region is not α-helical. This is tempting since the sequence Gly-His-Pro (which precedes E286) is found only in turns or loops in the eight proteins of known structure in which this sequence occurs (Hosler et al., 1993) (M. W. Calhoun, unpublished). If helix VI is, indeed, α-helical, the effect due to the E286A substitution must be indirect. In considering the splitting of the Cu_B–CO band due to the benign P293A mutation, this does not seem unlikely.

Tyrosine 288. The data presented in this work strongly indicate that substitutions for Y288 result in the loss of Cu_B. This is indicated both by the absence of the 2063 cm^{-1} Cu_B–CO FTIR band at 20 K and also by the rapid relaxation of the photolyzed CO at 135 K (Figure 7). This is similar to the effect of the substitutions for H284 (Calhoun et al., 1993c) and for H333 and H334 (Calhoun et al., 1993a). By the criterion of FTIR absorption difference spectroscopy, Cu_B is

either physically absent or, minimally, does not bind to CO. However, the requirement of H284, H333, and H334 for Cu_B insertion has also been observed by chemical analysis for copper bound to purified mutants of cytochrome bo_3 (Uno et al., 1994). Hence, it seems reasonable that the proper interpretation of the FTIR spectroscopy is that the Y288F, -H, -S, and -A mutants lack Cu_B. It previously has been noted that the effect of substitutions for both H284 and Y288 is qualitatively similar when one observed the CO recombination kinetics at room temperature (Brown et al., 1993). Substitutions for either H284 or Y288 substantially slow down that rate at which CO can diffuse through the protein to reach the high-spin heme o_3. This result is quite different from what is observed when either H333 or H334 is altered by mutagenesis (Brown et al., 1993; Lemon et al., 1993). Hence, although substitutions for H333, H334, H284, and Y288 all result in the absence of Cu_B, the state of the copper-less oxidase is not the same in each case. Indeed, the FTIR difference spectra of the Y288 mutants and the H284 mutants (Calhoun et al., 1993c) indicate that the environment in the vicinity of the heme Fe–CO adduct is considerably more ordered in the H284 mutants than in the Y288 mutants.

The important point is that the mutations at positions H333, H334, H284, and Y288 stand out insofar that Cu_B appears to be consistently absent from these mutants. This suggests the reasonable possibility that they may all be Cu_B ligands, if not simultaneously, then perhaps at different times during enzyme turnover. The model that has been proposed places all four of these residues in the immediate vicinity of Cu_B. Tyrosine ligation to copper has been demonstrated in galactose oxidase (Ito et al., 1991) and in copper-substituted lactoferrin (Smith et al., 1992), so that proposing Y288 as a Cu_B ligand seems biochemically reasonable, at least when considering precedents.

Spectroscopic data concerning the nature of the Cu_B ligands are equivocal. ENDOR studies of the mammalian oxidase suggest two or three histidines ligated to Cu_B (Cline et al., 1983) and as many as four histidines ligated to Cu_B in the ba_3-type oxidase from *Thermus thermophilus* (Surerus et al., 1992). EXAFS studies on the fully oxidized mammalian oxidase (Powers et al., 1981) and on the aa_3-type quinol oxidase from *Bacillus subtilis* (Powers et al., 1994) have been interpreted in terms of two histidine ligands plus one oxygen (or nitrogen) at a long distance (2.8 Å). In addition, one S or Cl is suggested to bridge between Cu_B and the high-spin heme Fe. Preliminary EXAFS studies have been performed using cytochrome bo_3 isolated in the absence of halide (R. A. Scott, J. O. Alben, J. Hill, J. Rumbley, and R. B. Gennis, unpublished). These experiments are not complete, but they should provide a critical test for the model proposed in Figure 9 in which Cu_B is ligated simultaneously to the three histidines and to Y288. It is noted that Y288, although very highly conserved, is not present in the subunit I sequences of all members of the heme–copper oxidase superfamily, notably, the cbb_3-type oxidases (van der Oost et al., 1994). Hence, it is likely that the protein residues in the immediate environment of Cu_B, or those that ligate to Cu_B, may differ in some members of the oxidase superfamily.

Modeling the Cu_B Ligation. Computer protein modeling of the Cu_B ligation suggests that all four residues mentioned above (H284, Y288, H333, and H334) can be favorably positioned to ligate Cu_B. The tyrosine–copper bond length in the model in Figure 9 represents a strong bond. Copper sites in proteins show that tyrosine may function either by short (ca. 2.0 Å), usually equatorial bonds (Smith et al., 1992) or by longer (ca. 2.6 Å), more axial or apical bonds (Ito et al., 1991). Although no attempt was made to model a longer bond with Y288, this is probably feasible. Although the model presented in Figure 9 is unlikely to be correct in terms of exact bond lengths or geometry, it is important to demonstrate that such a ligation scheme clearly is possible.

The models in Figure 9 show that H333 and H334 can provide chelation coordination to Cu_B perpendicular to the axis of helix VII. By assuming a helical structure for helix VI, H284 and Y288 are placed almost parallel to the helical axis and perpendicular to the H333 and H334 coordination sites. This arrangement of residues describes a potential tetrahedral coordination sphere (H_3YCu) that can produce a highly stable Cu(I) complex and, in turn, provide stability to the protein. Both theoretical and experimental approaches have been used previously to show that short protein sequences containing appropriate amino acid residues in favorable secondary structures can chelate transition metals such as copper (Arnold & Haymore, 1991). Specifically, in an α-helix, two metal-coordinating histidines separated by three other residues (HX_3H) is a favorable structure for metal binding (Arnold & Haymore, 1991). The pattern of the proposed ligands in helix VI corresponds to HX_3Y.

Molecular models and infrared spectra of the Cu_B–CO complex suggest that the copper coordination sphere is surrounded by nonpolar residues, which leads one to question how the local charge of the metal may be dissipated. Ionization of the tyrosinate (Y288) would provide an inner sphere charge compensation for Cu(I), further stablizing the complex, while the additional charge on Cu(II) may be accommodated by the ionization of a water molecule or carboxylate group. The latter does not appear to be available from a protein residue, but could make use of a heme propionate, perhaps as an outer sphere anion. The copper coordination sphere provides the flexibility to form either a tetrahedral or pentacoordinate (distorted tetrahedral or trigonal bipyramidal) complex. Molecular models suggest the latter for either $H_3YCu(I)$–CO (Figure 9A) or $H_3YCu(II)$–OH (not shown). The addition of carbon monoxide as a fifth ligand (Figure 9A) results in a trigonal bipyramidal geometry with reasonable CO-to-histidine ligand angles. Energy minimization placed the CO equally spaced between the three histidines and *trans* (axial) to the coordinated tyrosine oxygen. This simulated model is consistent with the time-resolved infrared linear dichroism observations, which estimated the $Cu_B(I)$–CO angle to be 51° with respect to mean heme plane (Dyer et al., 1989). Molecular models also suggest that coordination to H284 and Y288 rotates helix VI relative to helix VII, such that a flat surface is generated by helix VI, Cu_B, and helix VII. We suggest that this surface may be adjacent to the porphyrin ring of heme o_3.

Summary. The data presented in this paper provide additional evidence to support the conclusion based on previously reported data (Calhoun et al., 1993c; Hosler et al., 1993; Uno et al., 1994): that helix VI is adjacent to Cu_B and is on the distal side of the high-spin heme component of the binuclear center. Hence, the suggestion that Y288 might exchange with the high-spin heme axial ligand on the proximal side of the heme (Rousseau et al., 1993) seems unlikely. On the other hand, the possibility that Y288 might, at some point during the turnover of the oxidase, displace the heme axial ligand from the distal side (Einarsdóttir et al., 1993; Woodruff, 1993) is a possibility. The proposal that Y288 is a Cu_B ligand is chemically attractive in that the tyrosinate balances the internal charge of the copper. The experimental results of Dyer et al. (1989) mentioned above also add some credibility to the proposed model. Whether Cu_B is ligated to all four of

the proposed residues simultaneously and whether the specific ligation scheme suggested is correct remain to be determined. Clearly, all four are required for Cu_B to be bound stably to the protein. Furthermore, it seems very reasonable that one or more of these residues are likely to be involved directly in the proton pumping mechanism. In any event, it is hoped that the structural models presented here can provide a reasonable framework for the elucidation of mechanisms of oxidation and reduction coupled to energy conservation.

ACKNOWLEDGMENT

We thank Dr. Russ Hille for the use of his laboratory facilities and John Hill for assistance with the FTIR and discussions.

REFERENCES

Ahl, P. L., Stern, L. J., Düring, D., Mogi, T., Khorana, G., & Rothschild, K. J. (1988) *J. Biol. Chem. 263*, 13594–13601.

Arnold, F. H., & Haymore, B. L. (1991) *Science 252*, 1796–1797.

Brown, S., Rumbley, N. N., Moody, A. J., Thomas, J. W., Gennis, R. B., & Rich, P. R. (1993) *Biochim. Biophys. Acta* (in press).

Calhoun, M. W., Hill, J. J., Lemieux, L. J., Ingledew, W. J., Alben, J. O., & Gennis, R. B. (1993a) *Biochemistry 32*, 11524–11529.

Calhoun, M. W., Lemieux, L. J., Thomas, J. W., Hill, J. J., Goswitz, V. C., Alben, J. O., & Gennis, R. B. (1993b) *Biochemistry 32*, 13254–13261.

Calhoun, M. W., Thomas, J. W., Hill, J. J., Hosler, J. P., Shapleigh, J. P., Tecklenburg, M. M. J., Ferguson-Miller, S., Babcock, G. T., Alben, J. O., & Gennis, R. B. (1993c) *Biochemistry 32*, 10905–10911.

Chakrabarti, P. (1990) *Protein Eng. 4*, 57–63.

Chepuri, V., & Gennis, R. B. (1990) *J. Biol. Chem. 265*, 12978–12986.

Chepuri, V., Lemieux, L. J., Au, D. C.-T., & Gennis, R. B. (1990) *J. Biol. Chem. 265*, 11185–11192.

Cline, J., Reinhammar, B., Jensen, P., Venters, R., & Hoffman, B. M. (1983) *J. Biol. Chem. 258*, 5124–5128.

Consler, T. G., Tsolas, O., & Kaback, H. R. (1991) *Biochemistry 30*, 1291–1298.

Dyer, R. B., Einarsdóttir, O., Killough, P. M., López-Garriga, J. J., & Woodruff, W. H. (1989) *J. Am. Chem. Soc. 111*, 7651–7659.

Einarsdóttir, O., Dyer, R. B., Lemon, D. D., Killough, P. M., Hubig, S. M., Atherton, S. J., Lopez-Garriga, J. J., Palmer, G., & Woodruff, W. H. (1993) *Biochemistry 32*, 12013–12024.

Fiamingo, F. G., Altschuld, R. A., Moh, P. P., & Alben, J. O. (1982) *J. Biol. Chem. 257*, 1639–1650.

Fiamingo, F. G., Altschuld, R. A., & Alben, J. O. (1986) *J. Biol. Chem. 261*, 12976–12987.

Fiamingo, F. G., Jung, D. W., & Alben, J. O. (1990) *Biochemistry 29*, 4627–4633.

Henderson, R., Baldwin, J. M., Ceska, T. A., Zemlin, F., Beckmann, E., & Downing, K. H. (1990) *J. Mol. Biol. 213*, 899–929.

Hill, J., Goswitz, V. C., Calhoun, M., Garcia-Horsman, J. A., Lemieux, L., Alben, J. O., & Gennis, R. B. (1992) *Biochemistry 31*, 11435–11440.

Hill, J. J., Alben, J. O., & Gennis, R. B. (1993) *Proc. Natl. Acad. Sci. U.S.A. 90*, 5863–5867.

Holm, L., Saraste, M., & Wikström, M. (1987) *EMBO J. 6*, 2819–2823.

Hosler, J. P., Ferguson-Miller, S., Calhoun, M. W., Thomas, J. W., Hill, J., Lemieux, L., Ma, J., Georgiou, C., Fetter, J., Shapleigh, J., Tecklenburg, M. M. J., Babcock, G. T., & Gennis, R. B. (1993) *J. Bioenerg. Biomembr. 25*, 121–136.

Ishizuka, M., Machida, K., Shimada, S., Mogi, A., Tsuchiya, T., Ohmori, T., Souma, Y., Gonda, M., & Sone, N. (1990) *J. Biochem. (Tokyo) 108*, 866–873.

Ito, N., Phillips, S. E. V., Stevens, C., Ogel, Z. B., McPherson, M. J., Keen, J. N., Yadav, K. D. S., & Knowles, P. F. (1991) *Nature 350*, 87.

Kelly, M., Lappalainen, P., Talbo, G., Haltia, T., van der Oost, J., & Saraste, M. (1993) *J. Biol. Chem. 268*, 16781–16787.

Krab, K., & Wikström, M. (1978) *Biochim. Biophys. Acta 504*, 200–214.

Krebs, M. P., & Khorana, H. G. (1993) *J. Bacteriol. 175*, 1555–1560.

Lappalainen, P., Aasa, R., Malmström, B. G., & Saraste, M. (1993) *J. Biol. Chem. 268*, 26416–26421.

Lemieux, L. J., Calhoun, M. W., Thomas, J. W., Ingledew, W. J., & Gennis, R. B. (1992) *J. Biol. Chem. 267*, 2105–2113.

Lemon, D. D., Calhoun, M. W., Gennis, R. B., & Woodruff, W. H. (1993) *Biochemistry 32*, 11953–11956.

Minagawa, J., Mogi, T., Gennis, R. B., & Anraku, Y. (1992) *J. Biol. Chem. 267*, 2096–2104.

Minghetti, K. C., & Gennis, R. B. (1988) *Biochem. Biophys. Res. Commun. 155*, 243–248.

Minghetti, K. C., Goswitz, V. C., Gabriel, N. E., Hill, J. J., Barassi, C., Georgiou, C. D., Chan, S. I., & Gennis, R. B. (1992) *Biochemistry 31*, 6917–6924.

Powers, L., Chance, B., Ching, Y., & Angiolillo, P. (1981) *Biophys. J. 34*, 465–498.

Powers, L., Lauraeus, M., Reddy, K. S., Chance, B., & Wikström, M. (1994) *Biochim. Biophys. Acta 1183*, 504–512.

Puustinen, A., Finel, M., Virkki, M., & Wikström, M. (1989) *FEBS Lett. 249*, 163–167.

Puustinen, A., Finel, M., Haltia, T., Gennis, R. B., & Wikström, M. (1991) *Biochemistry 30*, 3936–3942.

Richardson, J. S., & Richardson, D. C. (1990) Principles and Patterns of Protein Conformation, in *Prediction of Protein Structure and the Principles of Protein Conformation*, Plenum Press, New York.

Rousseau, D. L., Ching, Y.-c., & Wang, J. (1993) *J. Bioenerg. Biomembr. 25*, 165–176.

Santana, M., Kunst, F., Hullo, M. F., Rapoport, G., Danchin, A., & Glaser, P. (1992) *J. Biol. Chem. 267*, 10225–10231.

Saraste, M. (1990) *Q. Rev. Biophys. 23*, 331–366.

Shapleigh, J. P., Hill, J. J., Alben, J. O., & Gennis, R. B. (1992a) *J. Bacteriol. 174*, 2338–2343.

Shapleigh, J. P., Hosler, J. P., Tecklenburg, M. M. J., Kim, Y., Babcock, G. T., Gennis, R. B., & Ferguson-Miller, S. (1992b) *Proc. Natl. Acad. Sci. U.S.A. 89*, 4786–4790.

Smith, C. A., Anderson, B. F., Baker, H. M., & Baker, E. N. (1992) *Biochemistry 31*, 4527–4533.

Solioz, M., Carafoli, E., & Ludwig, B. (1982) *J. Biol. Chem. 257*, 1579–1582.

Sone, N., & Hinkle, P. C. (1982) *J. Biol. Chem. 257*, 12600–12604.

Surerus, K. K., Oertling, W. A., Fan, C., Gurbiel, R. J., Einarsóttir, O., Antholine, W. E., Dyer, R. B., Hoffman, B. M., Woodruff, W. H., & Fee, J. A. (1992) *Proc. Natl. Acad. Sci. U.S.A. 89*, 3195–3199.

Thomas, J. W., Lemieux, L. J., Alben, J. O., & Gennis, R. B. (1993a) *Biochemistry 32*, 11173–11180.

Thomas, J. W., Puustinen, A., Alben, J. O., Gennis, R. B., & Wikström, M. (1993b) *Biochemistry 32*, 10923–10928.

Uno, T., Mogi, T., Tsubaki, M., Nishimura, Y., & Anraku, Y. (1994) *J. Biol. Chem. 269*, 11912–11920.

van der Oost, J., deBoer, A. P. N., deGier, J.-W. L., Zumft, W. G., Stouthamer, A. H., & van Spanning, R. J. M. (1994) *FEMS Microbiol. Lett. 121*, 109.

Wikström, M. (1977) *Nature 266*, 271–273.

Wikström, M., & Krab, K. (1979) *Biochim. Biophys. Acta 549*, 177–222.

Williams, K. A., & Deber, C. M. (1991) *Biochemistry 30*, 8919–8923.

Woodruff, W. H. (1993) *J. Bioenerg. Biomembr. 25*, 177–188.

Yun, C.-H., Wang, Z., Crofts, A. R., & Gennis, R. B. (1992) *J. Biol. Chem. 267*, 5901–5909.